buildings

MDPI

Article

Enhancing Compressive Strength in Cementitious Composites through Effective Use of Wasted Oyster Shells and Admixtures

Inyeong Cha, Jinwoong Kim and Heeyoung Lee *

Department of Civil Engineering, Chosun University, 309 Pilmun-Daero, Dong-Gu, Gwangju 501-759, Republic of Korea; ciy0814@chosun.kr (I.C.); daw220@chosun.kr (J.K.)
* Correspondence: heeyoung0908@chosun.ac.kr

Abstract: Wasted oyster shells generate environmental pollution and odor, thereby causing inconvenience to people. In addition, low-quality aggregates are generated owing to the lack of sand. To address these problems, cementitious composites that replaced sand with oyster shell powder were fabricated in this study, and a total 120 specimens were fabricated (specimen size: $50 \times 50 \times 50$ mm^3). The oyster shell substitution rate for sand, admixture type, and presence or absence of admixture were set as the experimental parameters. Herein, 0, 30, 70, and 100% of sand was replaced with oyster shell powder to examine the compressive strength of the cementitious composites according to the oyster shell powder content. The experiment results confirmed the decrease in the compressive strength of the cementitious composite with an increase in the oyster shell powder content. In the case of the cementitious composites mixed with oyster shell powder, silica fume, blast furnace slag, and an air-entraining water-reducing agent, the compressive strength increased by up to 30% with an increase in the oyster shell powder content. The results of cementitious composites containing oyster shell powder and admixture fabricated in this study indicate the potential of oyster shells as a new construction material that can replace sand.

Keywords: oyster shells; recycling; sand substitute; compressive strength; internal structure analysis

Citation: Cha, I.; Kim, J.; Lee, H. Enhancing Compressive Strength in Cementitious Composites through Effective Use of Wasted Oyster Shells and Admixtures. *Buildings* **2023**, *13*, 2787. https://doi.org/10.3390/buildings13112787

Academic Editor: Elena Ferretti

Received: 25 September 2023
Revised: 16 October 2023
Accepted: 3 November 2023
Published: 6 November 2023

1. Introduction

In Korea, approximately 280,000 tons of wasted oyster shells (WOS) are left unattended on the coast every year. During rains, the leachate from such WOS, which contains various foreign substances, flows through pipes to contaminate the ocean and land. In addition, WOS when left unattended for long periods, becomes a habitat for harmful larvae, and generates odor and environmental pollution, thereby causing inconvenience to people [1,2].

According to a report by the United Nations Environment Program (UNEP) [3] on the sustainability of sand, 50 billion tons of sand and gravel are used worldwide every year as construction materials. In Korea, an insufficient supply of aggregate renders construction difficult owing to the limited collection of marine aggregate and the reinforcement of the collection permit standards for land aggregate. The extraction of sand, which functions as an aggregate in marine ecology, renders protection against erosion, storms, and tsunamis difficult, and it causes risks to water supply, food production, fishing, and tourism industries. The significant loss of sand caused by coastal erosion has also occurred in Korea. Therefore, the long-term applicability of sand as a construction material must be considered.

The potential of WOS as an additive has been analyzed in many studies by preparing concrete and mortar. Yang et al. [4] verified that WOS has no significant impact on hydrates and only serves as a filler, even if it is mixed with cement paste, and demonstrated that the organic impurities included in WOS in small quantities do not cause harmful components of concrete. Ruslan et al. [5] reported that replacing certain amounts of aggregates in concrete with WOS increased compressive strength because a small amount of crushed WOS filled the existing voids. Li et al. [6] reported that adding WOS to bricks made of cement and fly

ash increased their strength and durability; moreover, there was an increase in durability owing to the addition of WOS under the effects of the freezing and thawing cycle of bricks. Wang et al. [7] prepared cement mortar by replacing fine aggregate with WOS and adding fly ash. The addition of WOS and fly ash filled the voids in the mortar, thereby decreasing water absorption and increasing compressive strength. Liao et al. [8] measured the compressive and flexural strengths of mortar according to the particle size of WOS; it was found that the compressive and flexural strengths of mortar increased, along with the increase in density, with a decrease in the WOS particle size. Naqi et al. [9] reported that crushed oyster shell (OS) powder rich in calcium oxides improved early compressive strength by enhancing the hydration reaction mechanism. Hong et al. [10] mixed the calcium ions separated from WOS with cement, prepared concrete, and measured the compressive strength. The concrete developed high early compressive strength, indicating that the calcium ions from WOS improved the compressive strength of the concrete. WOS can also contribute to addressing environmental problems in addition to improving compressive strength. Liao et al. [11] observed that sustainable and high-performance mortar can be produced if WOS is substituted for certain amounts of river sand mixed with mortar; it was also reported that WOS substitution for river sand significantly decreased CO_2 emissions compared with the typical mortar. Zhang et al. [12] mentioned that the absorption of CO_2 by organisms during the growth of OS is one of the carbon capture methods, and energy can be stored while achieving the goal of carbon capture if the CO_2 generated during the shell firing process can be collected and stored. Chen et al. [13] added fly ash or ground, granulated blast furnace slag (GGBS) to replace a certain amount of cement and prepared mortar by replacing the fine aggregate with crushed WOS; it was observed that the mortar mixed with fly ash and GGBS significantly reduced CO_2 emissions. Additionally, the study demonstrated that the mortar mixed with WOS and fly ash exhibited higher efficiency for the environment than that mixed with WOS and GGBS. However, WOS may have negative effects when added to mortar or concrete. Seo et al. [14] observed that the addition of calcined OS powder in large quantities negatively affected the compressive strength of concrete. In the study, the compressive strength of concrete decreased when the content of calcined OS powder exceeded 6% of the cement weight. Liu et al. [15] demonstrated that the mortar prepared by processing WOS with polyvinyl alcohol (PVA) and sodium silicate (SS) resulted in a reduction in compressive strength. However, this reduction can be improved using an admixture. Kjellsen et al. [16] conducted experiments on the inclusion of silica fume in concrete and paste production. In the early curings, specifically at day 1, the concrete and pastes containing silica fume exhibited similar or lower compressive strength than the specimens without silica fume. However, at 28 days, both the concrete and pastes with silica fume exhibited a significantly increased compressive strength than the specimens without silica fume. Toutanji et al. [17] reported that the use of silica fume, which is an admixture, contributed to the aggregate-matrix bond related to the formation of better interlock; it was reported that the use of silica fume and water-reducing agents increased the strength of mortar regardless of the water-to-cement (W/C) ratio. Ahmad et al. [18] incorporated silica fume and nylon fibers into recycled aggregate concrete (RCA). The experimental results indicated that concrete with the addition of silica fume and nylon fibers exhibited higher compressive strength than that without these additives. Concrete prepared with recycled aggregate typically experiences a reduction in compressive strength, but the inclusion of silica fume led to an increase in the compressive strength of the concrete. Siddique [19] observed that the addition of SiO_2, contained in silica fume, increased the compressive strength of the concrete cured for 28 days. In addition, the flexural strength increased as the SiO_2 substitution rate increased. Thus, the admixtures contributed to the compressive and flexural strengths of concrete. Huang and Feldman [20] prepared mortar by adding silica fume. When 30% of the cement weight was replaced with silica fume, the mortar cured for 90 days exhibited a high compressive strength of 77 MPa. In addition, the compressive strength of the mortar cured for 180 days was 82 MPa, indicating that the addition of silica fume was also favorable for long-term curing. Toutanji et al. [21] fabricated concrete

by incorporating silica fume, fly ash, and slag. In their study, it was observed that the highest compressive strength was achieved when the concrete contained 10% silica fume, 25% slag, and 15% fly ash. Oner and Akyuz [22] analyzed the compressive strength of concrete by incorporating GGBS. The initial compressive strength of GGBS concrete was lower than that of concrete without GGBS. However, as the curing days increased, the rate of increase in compressive strength became higher. This is attributed to the slow pozzolanic reaction associated with the incorporation of GGBS, which requires time for the formation of calcium hydroxide. Özbay et al. [23] reported that mortar mixed with GGBS increased the long-term compressive strength, wear resistance, and flexural strength, and that it also significantly reduced the concrete production cost. Köksal et al. [24] produced concrete by incorporating silica fume and steel fibers. The concrete produced with the inclusion of both silica fume and steel fibers exhibited higher compressive strength than that with only steel fibers or silica fume. This is because the inclusion of silica fume increases the compressive strength of concrete, enhancing its brittleness, whereas the addition of steel fibers increases the ductility of concrete. Johari et al. [25] prepared concrete by replacing cement with GGBS. At a GGBS substitution rate of 20%, concrete developed a maximum compressive strength of 110% compared with that of the control specimen. Therefore, the production of mortar using WOS and admixtures is expected to reduce the amount of WOS and the consumption of sand, a natural aggregate.

Previous investigations failed to demonstrate that cementitious composite incorporating WOS exhibited a compressive strength exceeding 40 MPa. Moreover, the introduction of WOS resulted in a decline in the compressive strength of the cementitious composite. Thus, this study fabricated cementitious composites by replacing sand with WOS. An admixture was also used to improve the compressive strength of the cementitious composites. The composites were prepared by varying the WOS content, presence or absence of the admixture added for strength improvement, and admixture type. The admixtures used included silica fume, blast furnace slag, and an air-entraining water-reducing agent (AE). The experimental parameters were composed of cementitious composites with no admixture, those mixed with silica fume and AE, and those mixed with blast furnace slag and AE (OS-Slag). The prepared specimens were cured for 7 and 28 days to analyze compressive strength and internal structure. To discern the cause of changes in the compressive strengths of the cementitious composites that used WOS, a field emission scanning electron microscope (FE-SEM), X-ray diffractometer (XRD), and thermogravimetric analyzer (TGA) were used in the internal structure analysis.

2. Experimental Program

2.1. Materials

Table 1 lists the mix proportions of the specimens. Ordinary Portland cement was used for cement, and silica sand no. 6 (sand size:0.35–0.7 mm) was used for sand. OSs from the southern coast of Korea were used, and OS powder was produced using a rock crusher. The produced OS powder was sifted through a #30 sieve (sieve opening: 600 μm) to obtain the same particle size as sand, and the particles that passed were used. Figure 1 shows the photograph of the crushed OS powder. Table 2 lists the chemical ingredients of the OSs. Silica fume, blast furnace slag, and AE that satisfied the ASTM C1240-20 [26], ASTM C989 [27], and ASTM C494 [28] regulations were used as the admixture and added to the cementitious composites containing OS powder. Table 3 lists the chemical ingredients of silica fume and blast furnace slag.

Table 1. Test parameters.

Test Unit Name	Sand (%)	Oyster Shell (%)	Cement (%)	Silica Fume (%)	Blast Furnace Slag (%)	AE (%)	W/C (%)
OS-0	100	0	100	0	0	0	30
OS-30	70	30					
OS-70	30	70					
OS-100	0	100					
OS-SF-0	100	0	100	15	0	0.5	30
OS-SF-30	70	150					
OS-SF-70	30	350					
OS-SF-100	0	500					
OS-Slag-0	100	0	100	0	15	0.5	30
OS-Slag-30	70	30					
OS-Slag-70	30	70					
OS-Slag-100	0	100					

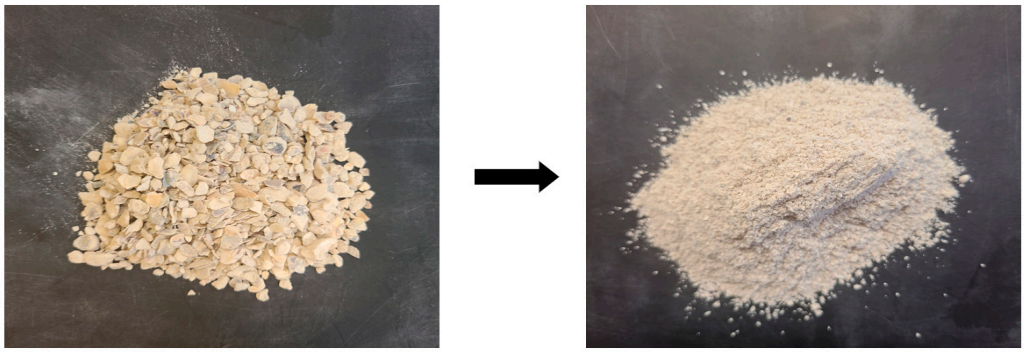

Figure 1. Process of manufacturing oyster shell powder.

Table 2. Chemical ingredients of oyster shells.

	$CaCO_3$ (%)	SiO_2 (%)	MgO (%)	P_2O_5 (%)	K (%)
OS	89.3	3.54	0.3	0.03	0.04

Table 3. Chemical ingredients of silica fume and blast furnace slag.

	SiO_2 (%)	Al_2O_3 (%)	Fe_2O_3 (%)	CaO (%)	MgO (%)
Silica fume	90.0	1.5	3.0	2.0	0.3
Blast furnace slag	31.12	14.24	0.51	41.40	6.14

2.2. Fabrication

The names of the experimental parameters were set according to the OS powder content and the presence or absence of an admixture. For example, the cementitious composite with an OS powder content of 0% and no admixture was set to OS-0, and that with an OS powder content of 100%, silica fume, and AE was set to OS-SF-100. AE was not indicated in the parameter names. The W/C ratio for the specimens was fixed at 0.3. The OS powder substitution rate for sand was increased from 0 to 30, 70, and 100%. In the experiment, the specimens were prepared with a size of 50 × 50 × 50 mm^3 in accordance with ASTM C109 [29] to test the compressive strength. Figure 2 displays the measurement of the compressive strength of a specimen. Figure 3 illustrates the experimental procedure. First, the weight of cement, sand, and OS powder was measured, as shown in Figure 3a. The materials were then placed in the bowl of the mixer and subjected to dry mixing for 5 min, as shown in Figure 3b. Cementitious composites were fabricated by adding water or

water and AE, and then mixing them for 3 min, as shown in Figure 3c. The specimens were cured in molds at a temperature of 25 ± 2 °C for 3 days, as shown in Figure 3d, and the compressive strength was measured. The curing period for the specimens was set to 7 and 28 days to measure the compressive strength at different ages.

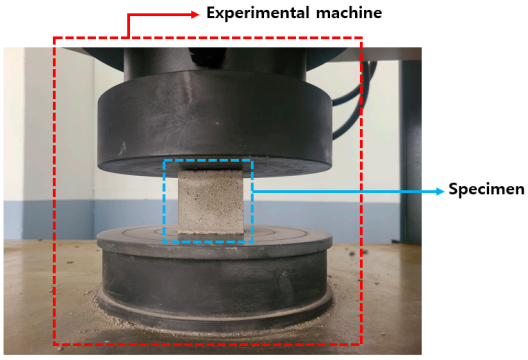

Figure 2. Compressive strength test setup.

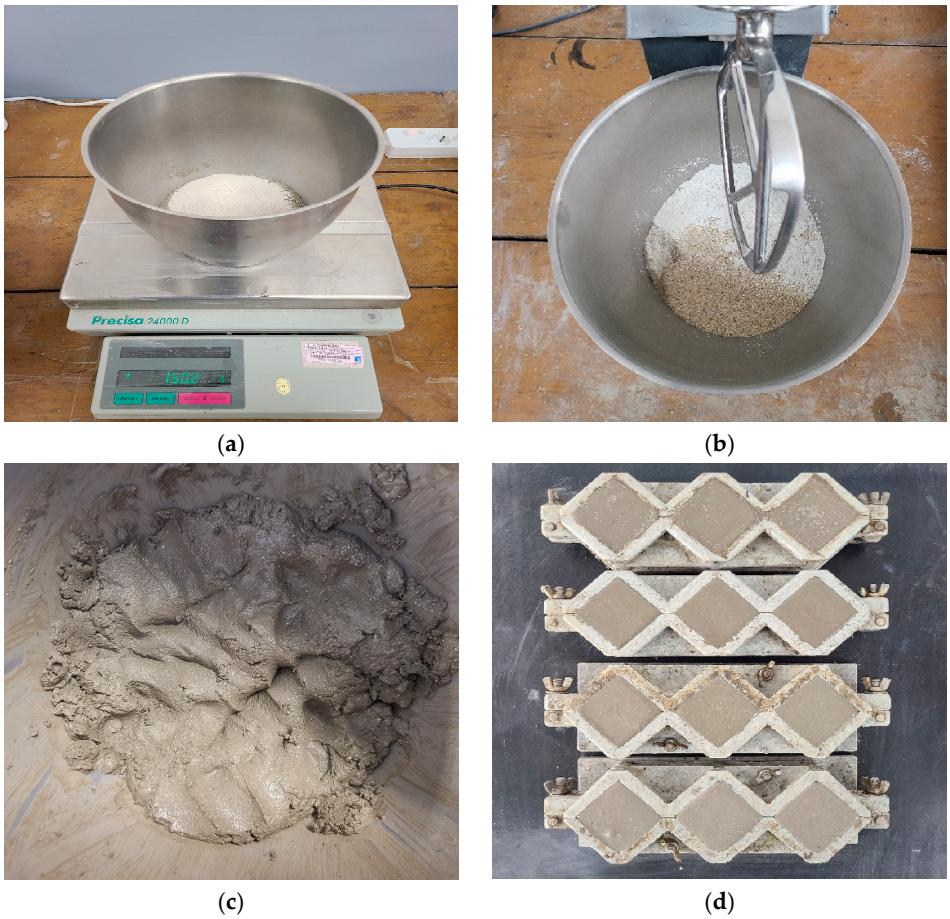

Figure 3. Fabrication process of mortar with oyster shells. (**a**) Weighing materials. (**b**) Dry mixing. (**c**) Mixing with water. (**d**) Curing mortar.

A total of 120 specimens were prepared by preparing five specimens for each parameter. The compressive strength was measured at a constant loading rate of 1 mm/min [30,31]. After analyzing the compressive strength, the specimens cured for 28 days were ground into powder using a rock crusher to analyze the microstructure of the cementitious composites. Figure 4a shows the prepared powder. FE-SEM analysis was conducted in accordance with ISO 19749:2021 [32], as shown in Figure 4b (Liu et al. [33]). The specimen surface

was observed at high magnification using the secondary electrons and the backscattered electrons generated via electron beam irradiation to the sample with FE-SEM. Figure 4c shows the XRD test setup. XRD was used in accordance with ASTM E915-96 [34–37]. In the XRD analysis, when the X-ray collides with a crystal, a portion of it is diffracted. Because the generated diffraction angle and strength are the unique values of the material structure, the types and quantities of the crystalline materials contained in the sample can be analyzed using X-rays. Figure 4d shows the TGA, which is an analyzer used to observe the weight fluctuations caused by the heat-induced chemical and physical changes of the sample according to time and temperature. TGA was used in accordance with ASTM C1872 [38]. When using TGA, a heat range of 20–600 °C and a heating rate of 10 °C/min were applied for the analysis (Liu et al. [39]).

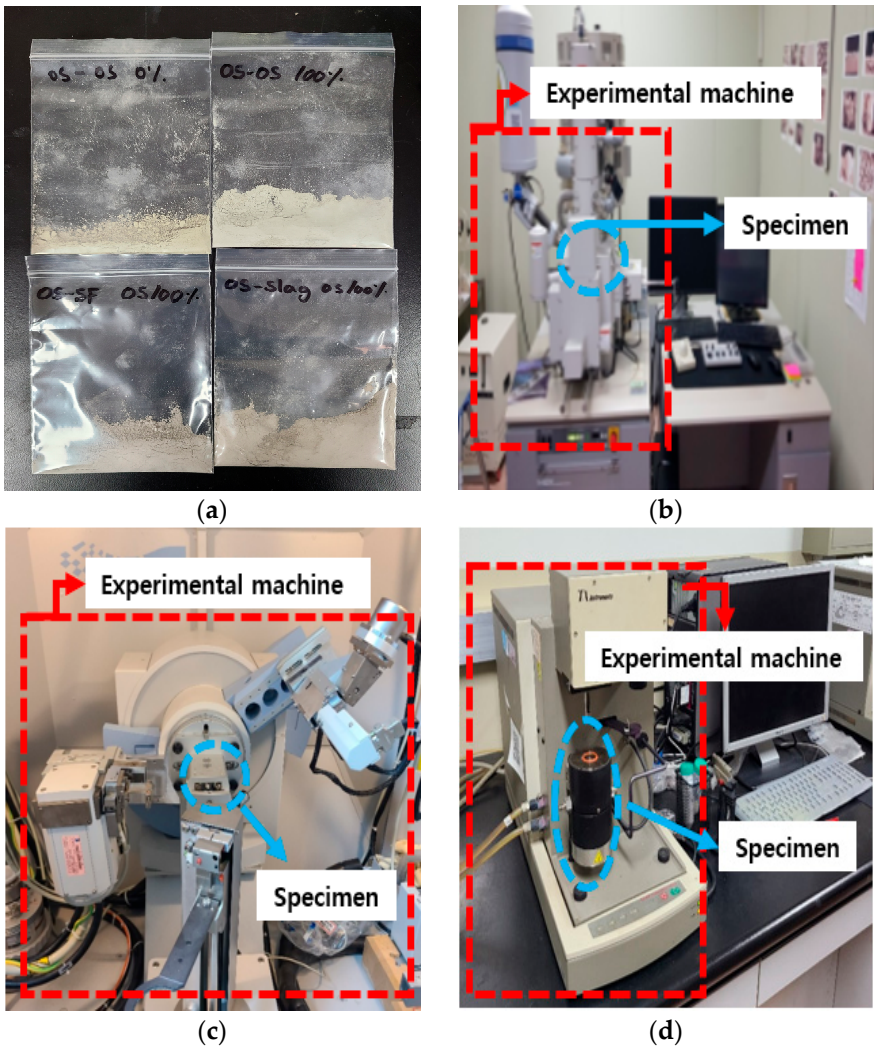

Figure 4. Internal structure analysis. (**a**) Specimen powder. (**b**) Field Emission Scanning Electron Microscope (FE-SEM). (**c**) X-ray Diffractometer (XRD). (**d**) Thermogravimetric analyzer (TGA).

3. Test Results

3.1. Compressive Strength Analysis of OS

The compressive strengths of the cementitious composite containing only OS powder after 7 and 28 days were analyzed. Figure 5a,b shows the compressive strength of OS after 7 and 28 days, respectively. After 7 days, the compressive strength of OS was observed to be 46.9 MPa for an OS powder content of 0%, 41.7 Mpa for 30%, 40.8 Mpa for 70%, and 38.4 Mpa for 100%. The compressive strength of OS-100 was approximately 18%

lower than that of OS-0. After 28 days, the compressive strength of OS was 49.2 Mpa for an OS powder content of 0%, 46.8 Mpa for 30%, 44.5 Mpa for 70%, and 42.6 Mpa for 100%. The compressive strength of OS-100 was approximately 13% lower than that of OS-0. The highest compressive strength of OS was observed from OS-0 cured for 28 days. The decrease in compressive strength of was observed with an increase in OS powder content. This can be attributed to the substitution of OS powder for silica sand in the cementitious composite, resulting in a reduction of SiO_2 content within the silica sand. As a consequence, the formation of calcium–silicate–hydrate (C-S-H) compounds in the cementitious composite was diminished, ultimately leading to a decrease in compressive strength. However, a compressive strength of more than 40 Mpa was developed even when 100% of the sand in the cement composite was replaced with OS powder. Therefore, it was concluded that Oss can be used as a new construction material that can replace sand in cementitious composites.

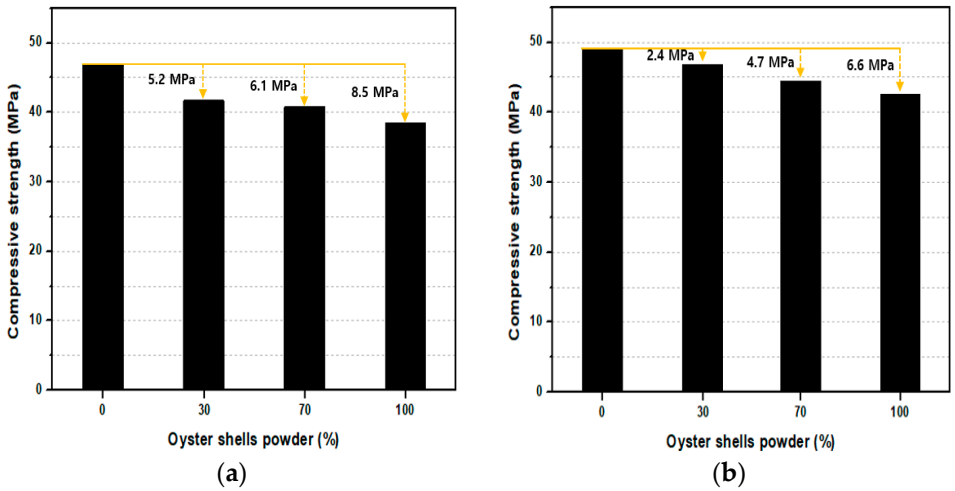

Figure 5. Compressive strength graph of OS according to oyster shells (OS) mixing ratio. (**a**) 7 days. (**b**) 28 days.

3.2. Compressive Strength Analysis of OS-SF and OS-Slag

As the addition of OS powder into cementitious composites decreased the compressive strength, additional specimens were prepared by adding both OS powder and admixtures to increase the compressive strength. Figure 6 shows the compressive strength of OS-SF, which was prepared using silica fume and AE as the admixture, according to the OS powder content and age. Among the OS-SF specimens, OS-SF-0 cured for 7 days exhibited the lowest compressive strength of 55.2 MPa. The compressive strength was observed to be 60.9 Mpa for OS-SF-30, 61.2 Mpa for OS-SF-70, and 63.7 Mpa for OS-SF-100. After 7 days, the compressive strength of OS-SF-100 was approximately 15% higher than that of OS-SF-0 with no OS powder. After 28 days, the compressive strength of OS-SF was 62.9 Mpa for OS-SF-0, 75.6 Mpa for OS-SF-30, 79.1 Mpa for OS-SF-70, and 82.3 Mpa for OS-SF-100. When cementitious composites were fabricated by adding OS powder, silica fume, and AE, a high strength of more than 80 Mpa was developed after 28 days. After 7 days, the difference in compressive strength between OS and OS-SF was 8.3 Mpa for an OS powder content of 0%, 19.2 Mpa for 30%, 20.4 Mpa for 70%, and 25.3 Mpa for 100%. After 28 days, the results were 13.7, 28.8, 34.6, and 39.7 Mpa, respectively. The specimens with an OS powder content of 100% exhibited the largest difference after both 7 and 28 days. This is because $CaCO_3$ in Oss contained in the cementitious composite and the SiO_2 contained in the silica fume of OS-SF caused more active C-S-H reactions at the same age. Therefore, the specimens with an OS powder content of 100% exhibited a larger compressive strength difference than those with 0%.

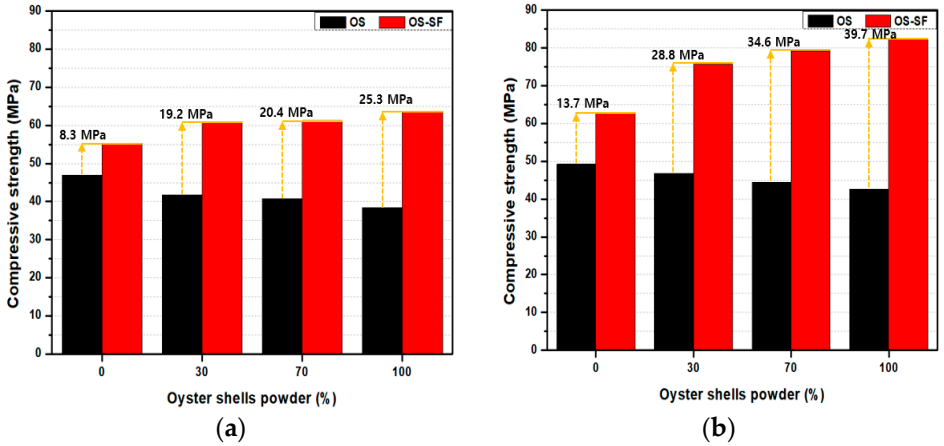

Figure 6. Compressive strength graph of OS-SF according to OS mixing ratio. (**a**) 7 days. (**b**) 28 days.

Figure 7 shows the compressive strength of OS-Slag, which was prepared using blast furnace slag and AE as the admixture, according to the OS powder content and age. The compressive strengths of OS-Slag after 7 days were 47.4, 51.5, 53.9, and 56.5 MPa for OS powder contents of 0, 30, 70, and 100%, respectively. For OS-Slag, the lowest compressive strength was also observed from the specimen with an OS powder content of 0% at 7 days, exhibiting the same tendency as OS-SF. The compressive strengths of OS-Slag after 28 days were 51.5, 52.6, 55.3, and 58.1 Mpa for OS powder contents of 0, 30, 70, and 100%, respectively. The largest compressive strength difference between OS and OS-Slag was 18.1 Mpa after 7 days and 15.5 Mpa after 28 days. In contrast, similar to OS-SF, OS-Slag exhibited induced C-S-H reactions, resulting in an enhancement of compressive strength. However, note that the increase in compressive strength observed in OS-Slag was relatively low when compared with OS-SF under similar conditions. This phenomenon can be attributed to the lower SiO_2 content in the blast furnace slag of OS-Slag in contrast with the high SiO_2 content present in the silica fume of OS-SF, which subsequently led to fewer C-S-H hydration reactions in OS-Slag. Table 4 presents the compressive strength of all the specimens.

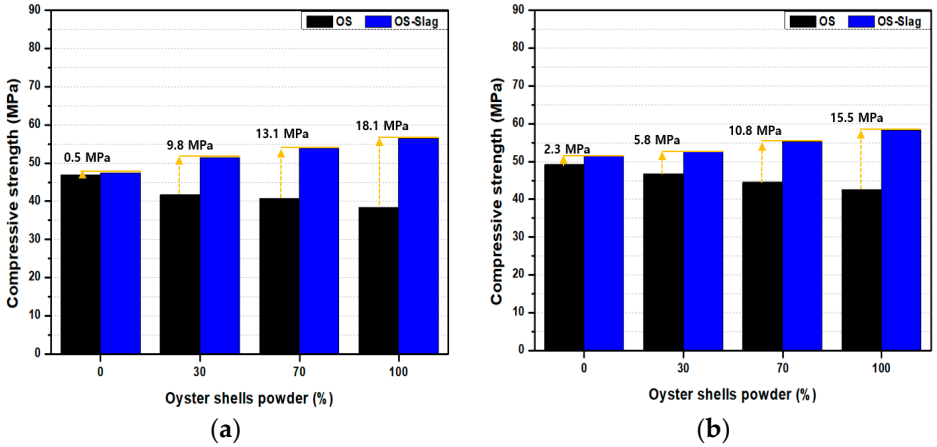

Figure 7. Compressive-strength graph of OS-Slag according to OS mixing ratio. (**a**) 7 days. (**b**) 28 days.

Table 4. Compressive strengths of the specimens.

Test Unit Name	OS/Cement Ratio (%)	7 Days (MPa)	28 Days (MPa)
OS-0	0	46.9	49.2
OS-30	30	41.7	46.8
OS-70	70	40.8	44.5

Table 4. *Cont.*

Test Unit Name	OS/Cement Ratio (%)	7 Days (MPa)	28 Days (MPa)
OS-100	100	38.4	42.6
OS-SF-0	0	55.2	62.9
OS-SF-30	30	60.9	75.6
OS-SF-70	70	61.2	79.1
OS-SF-100	100	63.7	82.3
OS-Slag-0	0	47.4	51.5
OS-Slag-30	30	51.5	52.6
OS-Slag-70	70	53.9	55.3
OS-Slag-100	100	56.5	58.1

3.3. Internal Structure Analysis

To discern the reason for the increase in the strength with the addition of an admixture into cementitious composites containing OS powder using FE-SEM, the internal structure of the cementitious composites cured for 28 days was observed. Figure 8a,b shows the FE-SEM images of OS-SF-100 and OS-Slag-100, respectively. The OS particles exhibited sharp geometry and formed flat and irregular layers. Thus, voids were formed owing to the insufficient binding effect between OS powder and fine aggregate, and the compressive strength of the specimen decreased with an increase in the OS powder content. However, such voids can be filled by adding silica fume and blast furnace slag. As shown in Figure 8a, a large amount of C-S-H generated via the addition of silica fume filled the voids between OS powder and sand. More voids than those in Figure 8a can be observed in Figure 8b because the blast furnace slag caused fewer C-S-H reactions than silica fume. Further, the C-S-H compounds can be observed to significantly decrease in Figure 8b compared with those in Figure 8a. Because silica fume generates more C-S-H hydrates than blast furnace slag and fills voids, the compressive strength of OS-SF improved more significantly than that of OS-Slag.

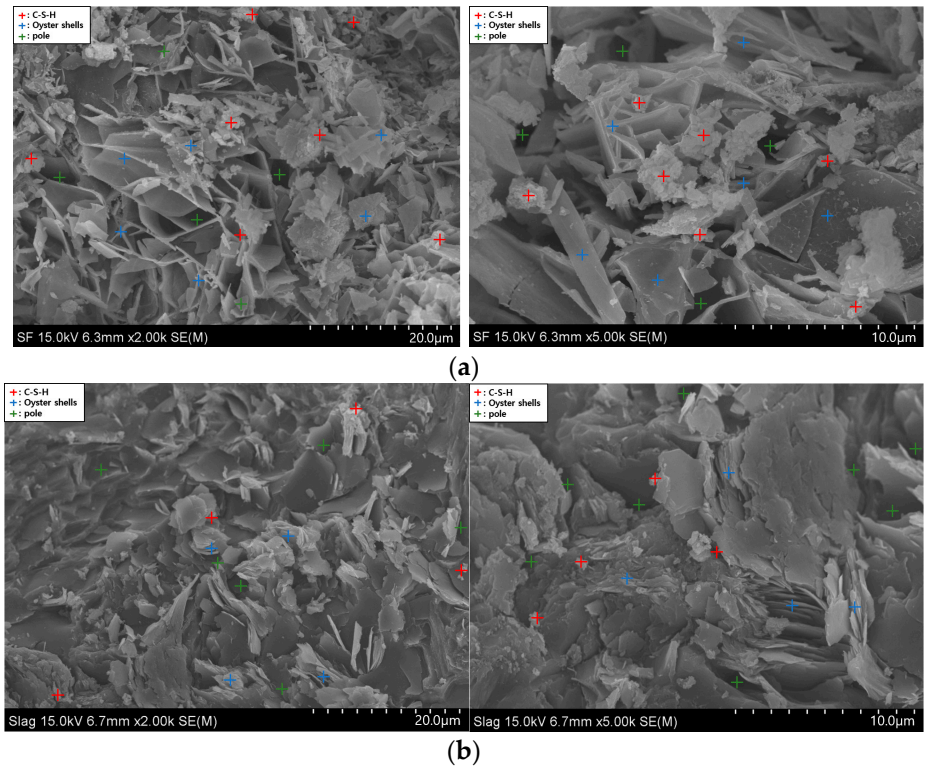

Figure 8. FE-SEM image of a specimen. (**a**) OS-SF. (**b**) OS-Slag.

XRD was performed to examine the internal materials of each specimen, and the results are shown in Figure 9. To identify the cause of the improvement in the compressive strength via the addition of admixtures, XRD analysis was conducted on OS-0, OS-100, OS-SF-100, and OS-Slag-100. $CaCO_3$, a component that forms C-S-H bonds, can be observed at approximately 30° and SiO_2 at approximately 26° and 50° in large quantities. The XRD analysis results indicated that $CaCO_3$ was included in all parameters; however, OS-0 included relatively less $CaCO_3$ because it did not contain OS powder and admixture. OS-100 and OS-SF-100 showed similar XRD graph patterns. This indicates that SiO_2 was used in the hydration reactions of OS-100 and OS-SF-100, thereby forming C-S-H bonds. However, OS-SF-100 contained a larger amount of SiO_2 than that in OS-100, owing to silica fume. Therefore, its compressive strength was improved because the amount of formed C-S-H compounds was larger than those in OS-100. OS-Slag was observed to contain a larger amount of non-reacting components than other parameters. This indicates the long-term strength improvement potential of OS-Slag, and OS-Slag is expected to be effective for long-term durability.

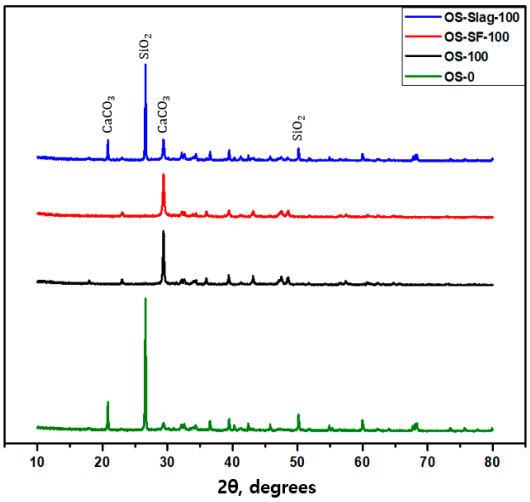

Figure 9. XRD analysis of a specimen.

To analyze the weight loss and mass change of OS-100, OS-SF-100, and OS-Slag-100 according to temperature, TGA was conducted, and the results are shown in Figure 10. All parameters exhibited the highest mass loss rate at the section from the initial temperature to 100 °C. OS-100 and OS-Slag-100 exhibited another rapid mass loss at approximately 450 °C. This phenomenon occurred owing to the dehydration of calcium hydroxide caused by heat. CH causes the additional strength of cementitious composites over time. More CH was generated in OS-Slag compared to OS-SF. This indicates that relatively long-term strength can be developed in OS-Slag compared to OS-SF. The mass loss rate began to rapidly decrease at approximately 500 °C. This indicates that OS powder, which was contained in all parameters, was subjected to the material decomposition process by heat at a temperature higher than 550 °C. At 600 °C, which is the highest temperature in the experiment, the mass loss rate was 8.8% for OS, 13.1% for OS-SF, and 7.7% for OS-Slag.

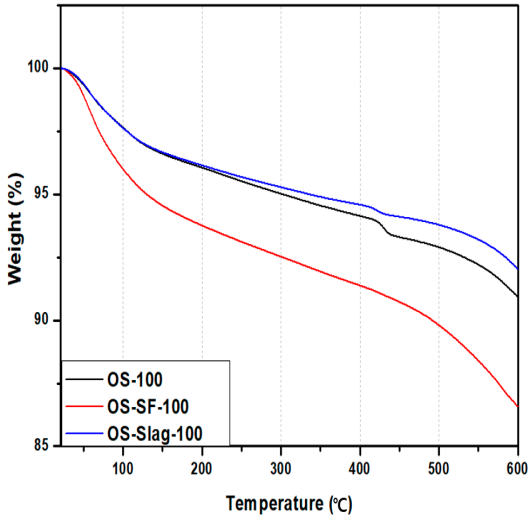

Figure 10. TGA analysis results.

4. Conclusions

In this study, cementitious composites were fabricated using OSs to replace fine aggregate. Silica fume, blast furnace slag, and an air-entraining water-reducing AE were added to improve the compressive strength of the cementitious composites. The compressive strength of the cementitious composites was measured after curing for 7 and 28 days. In addition, FE-SEM, XRD, and TGA were used to analyze the internal structure of the cementitious composites. The conclusions derived from this study are as follows:

(1) The compressive strength of the cementitious composite containing only OS powder tended to decrease as the OS powder content increased. The compressive strength of OS-100 was approximately 18% lower than that of OS-0 after 7 days and 13% lower after 28 days. The cement composite containing OS powder developed an average compressive strength of more than 40 MPa even without sand. Therefore, OSs are expected to be used as a new construction material that can replace sand.

(2) To improve the compressive strength that is reduced by the addition of OSs, cementitious composites were fabricated by adding admixtures. For both OS-SF and OS-Slag, the compressive strength increased as the OS powder content increased. The compressive strength of OS-SF-100 was up to 93% higher than that of OS-100, and the compressive strength of OS-Slag-100 was up to 36% higher than that of OS-100. This appears to be because SiO_2, one of the ingredients of the admixtures, reacted with $CaCO_3$ in OS powder and more actively generated C-S-H bonds. Based on this observed increase in compressive strength, future research endeavors will focus on investigating the flexural characteristics of cementitious composites incorporating wasted OSs and assessing their durability under environmental conditions.

(3) The FE-SEM analysis results indicated that SiO_2 in silica fume and $CaCO_3$ in OS powder generated a large amount of C-S-H compounds in OS-SF. C-S-H compounds were also generated in OS-Slag, but their quantity was smaller than OS-SF owing to the relatively low SiO_2 content compared to that in silica fume.

(4) The ingredients of OS-Slag-100 were identified in XRD and TGA analyses. The TGA results confirmed the formation of a large amount of CH in OS-Slag-100. The formation of CH accelerates further hydration by providing OS-Slag with a high alkaline environment. The XRD results also confirmed that many non-reacting materials were present in OS-slag, thereby causing fewer hydration reactions compared to other parameters during the same curing period. Therefore, OS-Slag is expected to have excellent characteristics for long-term strength, and further research will be conducted on long-term strength.

Author Contributions: Conceptualization, I.C. and H.L.; methodology, I.C.; formal analysis, J.K.; investigation, I.C. and J.K.; data curation, J.K.; writing—original draft preparation, I.C.; project administration, H.L. All authors have read and agreed to the published version of the manuscript.

Funding: This study was supported by a research fund from Chosun University, 2021.

Data Availability Statement: Not applicable.

Conflicts of Interest: The authors declare no conflict of interest.

References

1. Yoon, G.L.; Kim, B.T.; Kim, B.O.; Han, S.H. Chemical–mechanical characteristics of crushed oyster-shell. *J. Waste Manag.* **2003**, *23*, 825–834. [CrossRef]
2. Yang, E.I.; Kim, M.Y.; Park, H.G.; Yi, S.T. Effect of partial replacement of sand with dry oyster shell on the long-term performance of concrete. *Constr. Build. Mater.* **2010**, *24*, 758–765. [CrossRef]
3. United Nations Environment Programme. Sand and Sustainability: Finding New Solutions for Environmental Governance of Global Sand Resources. 2019. Available online: https://wedocs.unep.org/20.500.11822/28163 (accessed on 31 January 2023).
4. Yang, E.I.; Yi, S.T.; Leem, Y.M. Effect of oyster shell substituted for fine aggregate on concrete characteristics: Part I. Fundamental properties. *Cem. Concr. Res.* **2005**, *35*, 2175–2182. [CrossRef]
5. Ruslan, H.N.; Muthusamy, K.; Mohsin, S.M.S.; Jose, R.; Omar, R. Oyster shell waste as a concrete ingredient: A review. *Mater. Today Proc.* **2022**, *48*, 713–719. [CrossRef]
6. Li, G.; Xu, X.; Chen, E.; Fan, J.; Xiong, G. Properties of cement-based bricks with oyster-shells ash. *J. Clean. Prod.* **2015**, *91*, 279–287. [CrossRef]
7. Wang, H.Y.; Kuo, W.T.; Lin, C.C.; Po-Yo, C. Study of the material properties of fly ash added to oyster cement mortar. *Constr. Build. Mater.* **2013**, *41*, 532–537. [CrossRef]
8. Liao, Y.; Shi, H.; Zhang, S.; Da, B.; Chen, D. Particle size effect of oyster shell on mortar: Experimental investigation and modeling. *Materials* **2021**, *14*, 6813. [CrossRef] [PubMed]
9. Naqi, A.; Siddique, S.; Kim, H.K.; Jang, J.G. Examining the potential of calcined oyster shell waste as additive in high volume slag cement. *Constr. Build. Mater.* **2020**, *230*, 116973. [CrossRef]
10. Hong, M.; Jang, I.; Son, Y.; Yi, C.; Park, W. Agricultural by-products and oyster shell as alternative nutrient sources for microbial sealing of early age cracks in mortar. *AMB Express* **2021**, *11*, 11. [CrossRef] [PubMed]
11. Liao, Y.; Fan, J.; Li, R.; Da, B.; Chen, D.; Zhang, Y. Influence of the usage of waste oyster shell powder on mechanical properties and durability of mortar. *Adv. Powder Technol.* **2022**, *33*, 103503. [CrossRef]
12. Zhang, Z.J.; Liu, J.B.; Li, B.; Yu, G.X.; Li, L. Experimental study on factors affecting the physical and mechanical properties of shell lime mortar. *Constr. Build. Mater.* **2019**, *228*, 116726. [CrossRef]
13. Chen, D.; Zhang, P.; Pan, T.; Liao, Y.; Zhao, H. Evaluation of the eco-friendly crushed waste oyster shell mortars containing supplementary cementitious materials. *J. Clean. Prod.* **2019**, *237*, 117811. [CrossRef]
14. Seo, J.H.; Park, S.M.; Yang, B.J.; Jang, J.G. Calcined oyster shell powder as an expansive additive in cement mortar. *Materials* **2019**, *12*, 1322. [CrossRef]
15. Liu, R.; Chen, D.; Cai, X.; Deng, Z.; Liao, Y. Hardened properties of mortar mixtures containing pre-treated waste oyster shells. *J. Clean. Prod.* **2020**, *266*, 121729. [CrossRef]
16. Kjellsen, K.O.; Wallevik, O.H.; Hallgren, M. On the compressive strength development of high-performance concrete and paste—Effect of silica fume. *Mater. Struct.* **1999**, *32*, 63–69. [CrossRef]
17. Toutanji, H.A.; El-Korchi, T. The influence of silica fume on the compressive strength of cement paste and mortar. *Cem. Concr. Res.* **1995**, *25*, 1591–1602. [CrossRef]
18. Ahmad, J.; Zaid, O.; Pérez, C.L.C.; Martínez-García, R.; López-Gayarre, F. Experimental research on mechanical and permeability properties of nylon fiber reinforced recycled aggregate concrete with mineral admixture. *Appl. Sci.* **2022**, *12*, 554. [CrossRef]
19. Siddique, R. Utilization of silica fume in concrete: Review of hardened properties. *Resour. Conserv. Recycl.* **2011**, *55*, 923–932. [CrossRef]
20. Cheng-Yi, H.; Feldman, R.F. Influence of silica fume on the microstructural development in cement mortars. *Cem. Concr. Res.* **1985**, *15*, 285–294. [CrossRef]
21. Toutanji, H.; Delatte, N.; Aggoun, S.; Duval, R.; Danson, A. Effect of supplementary cementitious materials on the compressive strength and durability of short-term cured concrete. *Cem. Concr. Res.* **2014**, *34*, 311–319. [CrossRef]
22. Oner, A.; Akyuz, S. An experimental study on optimum usage of GGBS for the compressive strength of concrete. *Cem. Concr. Compos.* **2007**, *29*, 505–514. [CrossRef]
23. Özbay, E.; Erdemir, M.; Durmuş, H.İ. Utilization and efficiency of ground granulated blast furnace slag on concrete properties–A review. *Constr. Build. Mater.* **2016**, *105*, 423–434. [CrossRef]
24. Köksal, F.; Altun, F.; Yiğit, İ.; Şahin, Y. Combined effect of silica fume and steel fiber on the mechanical properties of high strength concretes. *Constr. Build. Mater.* **2008**, *22*, 1874–1880. [CrossRef]

25. Johari, M.M.; Brooks, J.J.; Kabir, S.; Rivard, P. Influence of supplementary cementitious materials on engineering properties of high strength concrete. *Constr. Build. Mater.* **2011**, *25*, 2639–2648. [CrossRef]
26. *ASTM C1240-20*; Standard Specification for Silica Fume Used in Cementitious Mixtures. ASTM International: West Conshohocken, PA, USA, 2020.
27. *ASTM C989*; Standard Specification for Slag Cement for Use in Concrete and Mortars. Annual Book of ASTM Standards. ASTM International: West Conshohocken, PA, USA, 2019.
28. *ASTM C494*; Standard Specification for Chemical Admixtures for Concrete. ASTM International: West Conshohocken, PA, USA, 2019.
29. *ASTM C109*; Standard Test Method for Compressive Strength of Hydraulic Cement Mortars (Using 2-in, or [50-mm] cube specimens). Annual Book of ASTM Standards. ASTM International: West Conshohocken, PA, USA, 2016.
30. Khurram, N.; Khan, K.; Saleem, M.U.; Amin, M.N.; Akmal, U. Effect of elevated temperatures on mortar with naturally occurring volcanic ash and its blend with electric arc furnace slag. *Adv. Mater. Sci. Eng.* **2018**, *2018*, 532406. [CrossRef]
31. Liu, S.; Zhang, Y.; Liu, B.; Zou, Z.; Liu, Q.; Teng, Y.; Zhang, L.V. Sustainable Use of Waste Oyster Shell Powders in a Ternary Supplementary Cementitious Material System for Green Concrete. *Materials* **2022**, *15*, 4886. [CrossRef]
32. *ISO 19749:2021*; Nanotechnologies—Measurements of Particle Size and Shape Distributions by Scanning Electron Microscopy. International Organization for Standardization: Geneva, Switzerland, 2021.
33. Liu, H.Y.; Wu, H.S.; Chou, C.P. Study on engineering and thermal properties of environment-friendly lightweight brick made from Kinmen oyster shells sorghum waste. *Constr. Build. Mater.* **2020**, *246*, 118367. [CrossRef]
34. *ASTM E915-96*; Test Method for Verifying the Alignment of X-Ray Diffraction Instrumentation for Residual Stress Measurement. ASTM International: West Conshohocken, PA, USA, 2002.
35. Tony, V.C.S.; Voon, C.H.; Lee, C.C.; Lim, B.Y.; Gopinath, S.C.B.; Foo, K.L.; Arshad, M.K.M.; Ruslinda, A.R.; Hashim, U.; Nashaain, M.N.; et al. Effective synthesis of silicon carbide nanotubes by microwave heating of blended silicon dioxide and multi-walled carbon nanotube. *Mater. Res.* **2017**, *20*, 1658–1668. [CrossRef]
36. Singh, S.; Khan, S.; Khandelwal, R.; Chugh, A.; Nagar, R. Performance of sustainable concrete containing granite cutting waste. *J. Clean. Prod.* **2016**, *119*, 86–98. [CrossRef]
37. Luo, J.; Chen, X.; Crump, J.; Zhou, H.; Davies, D.G.; Zhou, G.; Zhang, N.; Jin, C. Interactions of fungi with concrete: Significant importance for bio-based self-healing concrete. *Constr. Build. Mater.* **2018**, *164*, 275–285. [CrossRef]
38. *ASTM C1872*; Standard Test Method for Thermogravimetric Analysis of Hydraulic Cement. ASTM International: West Conshohocken, PA, USA, 2018.
39. Liu, S.; Wang, Y.; Liu, B.; Zou, Z.; Teng, Y.; Ji, Y.; Zhou, Y.; Zhang, L.V.; Zhang, Y. Sustainable utilization of waste oyster shell powders with different fineness levels in a ternary supplementary cementitious material system. *Sustainability* **2022**, *14*, 5981. [CrossRef]